Meccanica (2022) 57:2117–2130
https://doi.org/10.1007/s11012-022-01540-6

Operation extension in gas turbine-based advanced cycles with a surge prevention tool

Federico Reggio · P. Silvestri · M. L. Ferrari · A. F. Massardo

Received: 18 October 2021 / Accepted: 17 May 2022 / Published online: 11 June 2022

Abstract This work aims to present the development and testing of an innovative tool for surge prevention in advanced gas turbine cycles. The presence of additional components, such as a saturator in humid cycles, a heat exchanger for an external combustor, a solar receiver or fuel cell stack in a hybrid system, implies the presence of larger size volumes between compressor outlet and recuperator or expander inlet. This large volume increases the risk of incurring in surge instability, especially during dynamic operations. For these reasons, at the University of Genoa, the Thermochemical Power Group (TPG) has implemented four surge precursors in a new diagnostic real-time software which can recognise a surge incipience condition comparing the precursor values with a set of moving thresholds. The most innovative aspects of this work are: (i) operational range extension and safer management of advanced gas turbine systems for energy generation, (ii) positive impact in energy efficiency due to this range extension of high efficiency systems, (iii) development of a new diagnostic tool for surge prevention using standard probes, (iv) small impact of this tool on the control and sensor costs, (v) software flexibility for adaptation to different conditions and machines. This very important final aspect is obtained with thresholds able to change automatically to adapt themselves to the plant and machine operational regime. From the cost point of view, the utilization of standard measurements is an essential requirement to equip commercial machines without significant impact on the capital costs. The software performance has been demonstrated using experimental data from a test rig composed of a T100 microturbine connected with a modular vessel, which permits to generate the effect of additional components (especially from the volume size point of view). Vibro-acoustic data, collected during machine transients from a stable operative condition to surge, were used to tune all the software parameters and to obtain a good surge predictivity.

Keywords Surge prevention · Gas turbine · Advanced cycle · Vibro-acoustic · Large volume

List of symbols

Variables	FO	Fractional opening [%]
Kp		Surge margin [−]
M		Mass flow rate [kg/s]
N		Rotational speed [rpm]
TOT		Turbine outlet temperature [K]
β		Pressure ratio [−]
TC1		Compressor inlet temperature [K]
Acronyms	CSP	Concentrated solar power
STIG		STeam injected gas turbine
E. grid		Electrical grid
Ex		Heat exchanger

F. Reggio (✉) · P. Silvestri · M. L. Ferrari · A. F. Massardo
Thermochemical Power Group (TPG), Università degli studi di Genova, Genoa, Italy
e-mail: federico.reggio@edu.unige.it

HAT	Humid air turbine
REC	RECuperator
REF	REFormet
RMS	Root mean square
SOFC	Solid oxide fuel cell
TPG	Thermochemical power group
mic	MICrophone
acc	ACCelerometer
var	VARiance
ref	REFerence
AD	Angle domain
fft	Fast fourier transform
sub	SUB synchronous
Spe	SPEctrum
VBE	Emergency bleed valve

1 Introduction

Advanced cycles based on gas turbine technology show significant benefits or promising aspects to face the issues of current and future energy scenarios [1]. Especially good performance in terms of high efficiency [2], low pollution [3] and possible applications with renewable sources [4] is an important response to energy demand increase and environmental impact problems [5]. Some turbine-based plant layouts (involving researchers during the last 20–30 years) are not commercial solutions due to both economic and technology constraints [6]. Examples of this aspect can be shown considering hybrid systems based on high temperature fuel cells [7] or Humid Air Turbine (HAT) systems [8]. However, different advanced cycles have reached the commercial level, such as recuperated turbines [9], STeam Injected Gas turbine (STIG) systems [10] or externally fired machines (e.g. turbines fuelled with biomass combustion) [11]. Moreover, research activities involve gas turbines for further applications, such as in concentrated solar power systems [12] or in innovative layouts including energy storage devices [13]. All these advanced cycles based on gas turbine technology include additional components in comparison with the simple cycle layout generating a significant volume size increase between the compressor and the expander [14]. This volume increase ranges from a limited amount (e.g. the volume of recuperator ducts [15]) to values higher than two orders of magnitude (e.g. the fuel cell size in hybrid systems [16]). Although the additional volume has a limited effect on the steady-state performance (from negligible to a small increase of pressure and thermal loss depending on the additional component type), its impact on the dynamic behaviour is significant [17]. The increase in pressurisation/depressurisation time coupled to specific operational behaviour and constraints of the additional components (e.g. operations to maintain the fuel cell temperatures as constant as possible) has an important impact on system dynamic performance and control system issues. For instance, some authors [16] presented the necessity to modify the turbine control system to avoid surge during the shutdown operation in systems connected to large volumes, due to the increased depressurisation time.

In this scenario, surge prevention in gas turbine-based advanced cycles is an important aspect to be investigated from both an academic and an industrial point of view because vibrations due to surge can damage plant mechanical components [18]. Regarding surge subject, the authors suggest C. Cravero's Computational Fluid Dynamics papers [19, 20], G.L. Arnulfi's experimental and numerical works [21, 22] and E.M. Greitzer's works [23]. Since commercial machines are not equipped with surge prevention tools/devices and compressor maps are not reliable for such diagnostic operations, the development of surge prevention techniques for real-time application is mandatory for the commercialisation of these advanced cycle gas turbines.

Although previous works [24–26] were published on surge precursor topics, this paper extends the concept presenting new software for surge prevention in real-time mode. Moreover, considering the most advanced papers [27, 28] or patents [29] on this topic, no previous activities combined different precursors and/or presented a detection tool based on an adaptable threshold. So, the novelty of this work mainly consists of:

- Important performance improvement in terms of applicability of advanced cycles based on gas turbine technologies (due to the possibility of operations closer to the surge line);
- Significant efficiency increase for energy generation due to larger applications of advanced gas turbine based cycles (e.g. hybrid cycles including a fuel cell);

- Standard probes based innovative tool for real time diagnostic (surge prevention);
- Important benefit, from cost point of view, due to easy integration with standard control tools;
- High flexibility performance in terms of software adaptation to different operative conditions and machines.

Although the software for surge prevention presented in this work is flexible for applications in advanced cycles of different size, the results of this paper were obtained with a T100 microturbine [16]. This application was motivated considering the interest in small size plants for distributed generation [30] especially in very high efficiency layouts (e.g. fuel cell-based hybrid systems), and the availability of a T100-based rig including a large size additional volume [16]. However, this does not limit the software applications to large size gas turbines or turbochargers. Hence, the Thermochemical Power Group (TPG) of the University of Genoa used the mentioned test rig to compare different volume size configurations and to demonstrate the effectiveness of the diagnostic tool in surge-approaching detection. For this reason, it is also important to highlight the innovative aspect regarding the software flexibility that was demonstrated considering three different volume size conditions. In all cases, the tool was able to produce a signal related to the detection of surge approaching on the basis of four different precursors, considering the techniques developed in previous steps of this activity [14].

2 Surge risk with large volume components

Gas turbines based on advanced cycle layouts (for efficiency increase reasons or better exploitation of renewable sources) are usually equipped with large volume components installed in the pressurised zone (between compressor outlet and turbine inlet). Typical examples of these layouts are shown in Fig. 1 where the large volume components are highlighted: (i) the furnace in the externally fired gas turbine [31], (ii) the solar receiver in the Concentrated Solar Power (CSP) turbine [32], (iii) the saturator in the Humid Air Turbine (HAT) [33], and (iv) the fuel cell in the hybrid system [34]. Moreover, other layouts, such as turbines with recuperator or intercooler, include additional volume due to heat exchanger ducts. However, its impact might be negligible due to the small amount of additional volume.

This additional volume generates important changes in the dynamic behaviour due to the different response of pressurisation/depressurisation. Moreover, the impact of this volume depends on its size, ranging from almost negligible change (in case of connection with heat exchangers) to important dynamic behaviour modifications with large vessels (i.e. a fuel cell). For this reason, the commercial control systems designed for standard gas turbines might be unable to prevent risky situations, such as surge events, during dynamic conditions. A specific example could be shown considering the shutdown phase of a T100 microturbine connected to a large volume vessel: during this transient, the standard control

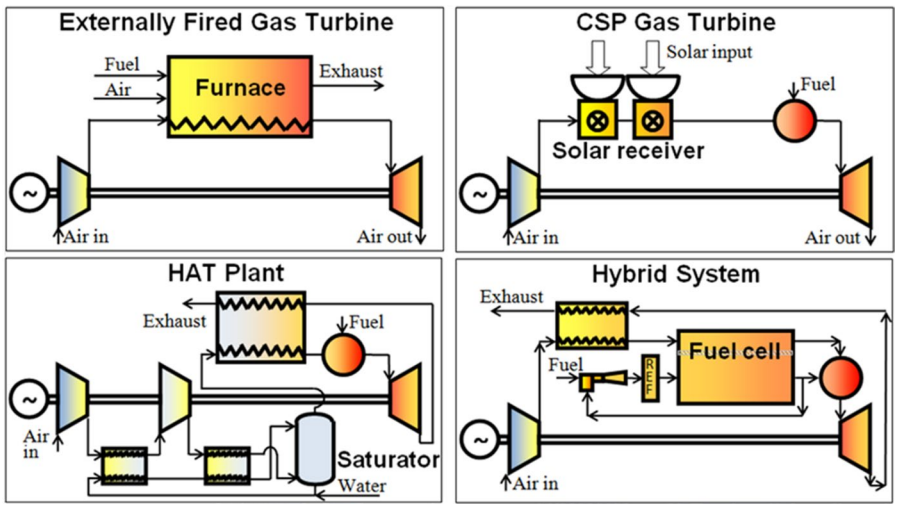

Fig. 1 Some layouts of gas turbines based on advanced cycles

system of the TPG laboratory microturbine was not able to prevent the surge unless a bleed valve opened (knowledge obtained with several preliminary tests). The development of general surge prevention techniques is therefore an important added value for gas turbines based on advanced cycles to avoid operational field and efficiency decrease due to a necessary higher distance from the surge line. Especially for the cases with larger volume sizes, such as fuel cell-based hybrid systems, the missing techniques for surge prevention is one of the factors that is limiting the market penetration perspectives of these kinds of systems [16]. Moreover, these techniques have to be based on: reliable and standard sensors, acceptable cost increase for the machine requirements, and implemented in real-time software for the integration with the control tool.

To conclude this section, it is important to mention gas turbines connected to large volume devices for energy storage reasons. Possible examples of energy storage systems responsible for volume size increase could be: compressed air vessels [35], devices based on high temperature materials [36] or systems based on thermo-chemical reactions [37]. In all these cases the volume size increase has a significant impact on the dynamic behaviour change justifying the development of these real-time surge prevention techniques.

3 Test rig

The vibro-acoustic experimental results presented in this paper were obtained with a T100 microturbine coupled with external vessels (the plant layout shown in Fig. 2) [16]. This configuration is due to the original purpose of the test rig: an emulator plant for experimental activities on SOFC based hybrid systems [16]. So, the vessels are: a modular device designed to emulate the cathodic side and a 0.8 m^3 vessel for the anodic side. The total size available as additional volume (including the pipes) is about 4.1 m^3. While the T100 turbine is able to produce 100 kW in nominal conditions (at 70,000 rpm), in this experimental plant it is not possible to produce more than 73.5 kW at 300 K of compressor inlet temperature. This is due to the additional pressure drop (about 142 mbar) and temperature losses (about 99 K) related to the external devices [14].

The rig is also equipped with different devices: air/water heat exchangers to control the compressor inlet temperature (TC1), an emergency bleed valve (VBE), which are control valves to manage the air flows, accelerometers and microphones (as shown in Fig. 2) for the vibro-acoustic measurements [14], measurement probes (for mass flow, pressure, temperature and rotational speed) connected to the T100 control system or to the acquisition/control software developed in LabVIEW™. Since the technical details were reported in previous works [14]16, no further plant data are presented for the sake of brevity.

4 Software description

A new diagnostic software for surge prevention has been developed in LabVIEW programming language: it is based on some predictors obtained

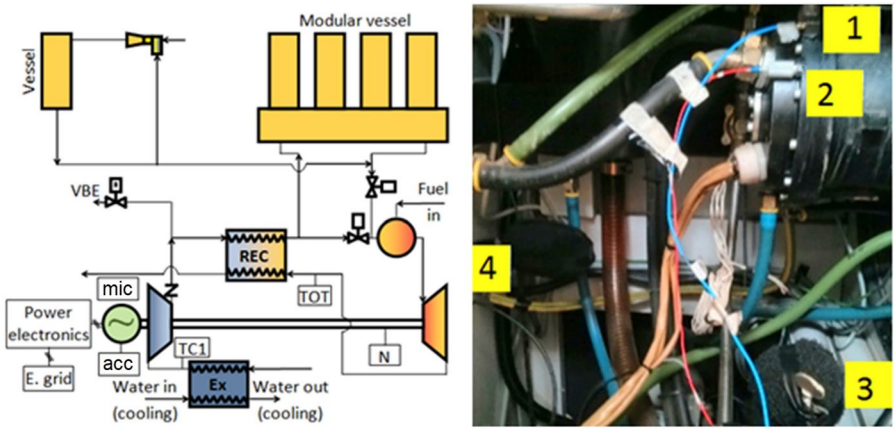

Fig. 2 Test rig layout and location of sensors for vibro-acoustic measurements: **1** tri-axial sensor, **2** mono-axial accelerometer with higher amplitude range, **3** radial microphone, **4** axial microphone

during the analysis of vibrational and acoustic data [38] acquired in previous experimental campaigns [14, 39].

Four surge precursors are implemented and calculated from data acquired in real-time mode considering their RMS values: (i) accelerometer and (ii) sub-synchronous microphone, (iii) sub-synchronous variance spectrum and (iv) angle domain analysis [14, 39]. The four functions for the precursor calculation are included in the software main tool which collects vibro-acoustic data from an accelerometer, a microphone and a tacho signal and which gives in real-time mode (as outputs) some warnings that indicate if the plant works in a stable or surge incipience condition. The software main loop receives three windows of signals every half a second; these three intervals of signal last 5 s. This means that each new window of 5 s enters in cycle loop differing, compared to the previous one, by an interval of half a second of new data and keeping 4.5 s of old data. The length of 5 s has been chosen to provide a good frequency resolution during the calculation of precursors since they consider the presence of sub-synchronous contents in the signals, while the time step of half a second has been chosen to follow the dynamic of the plant (it can be changed as a parameter of the software).

Figure 3 shows the main loop scheme of the software zooming in on the accelerometer input in order to explain how the signal enters the main loop.

Every half a second from the 3 vibro-acoustic signals the 4 precursors are calculated and each one is compared to a corresponding reference value obtained from the values of precursors in the past. This is based on the "maximum time distance" parameter that represents the reference values updating period. During this period each current value of the precursors is compared with its own reference value that is kept constant. The reference values, one for each precursor, are updated every "maximum time distance" period and obtained from a matrix of previous values. The values of the reference are calculated considering the median value of each set (columns) in the matrix. The median value has been preferred over the average due to its ability to weigh less possible anomalous peaks inside the data in the matrix columns.

This kind of moving threshold for the precursor values, which considers older values, has been chosen to maximise the range of applicability of the software. If the thresholds were constant, it would be useful only for one specific plant and for one specific regime of the machine. Using a threshold which is the average from a set of values obtained some seconds

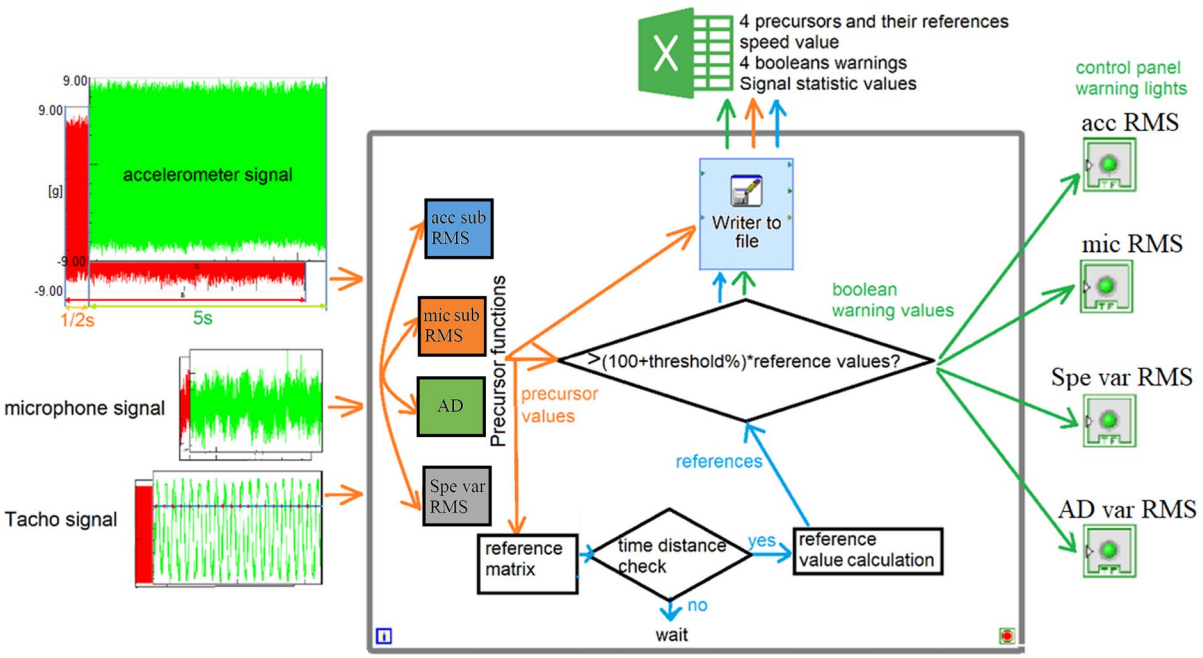

Fig. 3 Software input/output layout

before the actual value means obtaining a reference that identifies the plant and machine status/regime. This threshold allows to check if there are some status changes referring to the surge for any plants and machine regimes. If a precursor exceeds its reference value by a percentage settable by the user, a single warning is given. If three or four warnings are given, it can be considered as an alarm of surge approaching.

Four groups of parameters are defined for the control of the functions which calculate the precursors: these functions and their parameters are described in the next paragraph. In addition to the four percentages needed to compare the actual precursor values with their corresponding references, the user can set three parameters: the maximum time distance between the actual precursor values and the relative reference values, the automatic variation of this maximum and number of values in the matrix for the reference calculations.

The first parameter is called "maximum time distance" because, once the main function has calculated the four reference values, the software compares all the new precursors every half a second to those values until the maximum time distance is reached (when other references are obtained). This maximum time distance can be constant or automatically corrected. The second parameter is the time variation for the automatic correction of the aforementioned maximum time distance from the reference. If the user sets a time variation higher than zero, every time the software calculates the new reference values it compares them with the precedent reference values. If the value of the sum of the new references (non-dimensional values) is higher than the value of the sum of the old ones, the maximum time distance is increased by the value of the time variation; if it is lower the time distance is reduced, otherwise it is kept constant. Increasing the time variation (and/or the "maximum time distance") could increase the warning sensitivity to the precursor variation: if the time trend of a precursor has a slow (but positive) slope, increasing the "maximum time distance" from the reference values means waiting for some additional seconds with the same threshold values. During this increased period, if precursors increase more than the chosen reference percentages the warnings are activated.

The third parameter is the number of values for each precursor to be kept in the matrix for the calculation of the references.

All three of these parameters are expressed in the form of a number of half seconds and the second two parameters must be lower than the initial value of the maximum distance from the reference. These last three parameters and the percentages for the comparison affect the diagnostic capacity of the software. For example, the time variation must be small to avoid excessive variation of the maximum time distance, which should be long enough to refer to a more stable condition, but not excessive to refer to a too different machine regime. If the parameters produce an excessive sensibility of the system to low variation of the precursors, the software can have as output false alarms, meanwhile too low a sensitivity can reduce its surge prevention capability. For this reason, a tuning process has been carried out to obtain a good default parameter set for the software. It will be described in the "Software tuning and results" section of this paper.

5 Surge precursor functions

This section describes the four surge precursors (preliminarily presented in previous works [14, 39]) implemented in the software.

The first two precursors are the RMS values of the filtered microphone and the accelerometer signals. They are calculated by a similar sub function which takes the signal input window, filters it in the sub-synchronous field and then divides the signal into some sections from which it calculates some RMS values and their mean. Figure 4 shows the scheme for one of these precursor calculations: in this process, the user can set the parameters of a Butterworth filter and the time interval used to divide the signal into sections to obtain a set of RMS values for the mean. For the software testing, shown in the next section of the paper, the filter was set as a pass band filter of 100th order between 5 and 800 Hz, while the section length for the mean was set to 1 s. The range of frequencies and the order of the filter was chosen to obtain similar results to those obtained in the past analysis [14, 39], while 1 s section length allows to keep a good frequency resolution in the signal (1 Hz) and to have a mean of 5 RMS values. The filter order is high to increase the slopes at the cut off frequencies, but the signal phase changes because the filter has not to affect its RMS value.

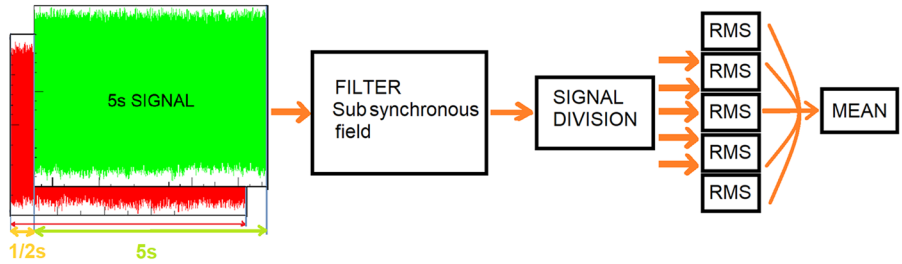

Fig. 4 Sub-synchronous RMS precursor calculation scheme: if the section length for the mean is 1 s, 5 RMS values are calculated for the mean

The third precursor implemented in the software is the RMS value of the auto-power spectrum variance in the sub-synchronous field; it indicates a lack of stationarity in the accelerometer signal from a spectrum point of view. Figure 5 shows the scheme for this precursor calculation: the sub function divides the 5 s input signal into some intervals; from these intervals the software obtains a set of auto power spectra which are arrays of energy values, each value corresponding to a frequency of the spectrum. Then, the software calculates the variance considering the mean of the energy values for each frequency from each array: this means obtaining a new array whose elements are the variance of the signal energy for every frequency (auto-power spectrum variance). Once the array of the variance spectrum has been obtained, the relative surge precursor is calculated obtaining the RMS of the values in the range between those corresponding to the considered sub-synchronous limit frequencies. For the software testing the 5 s signal was divided into 20 intervals lasting a quarter of second: so, the calculated spectra had a frequency resolution of 4 Hz, considered enough in comparison to the sub-synchronous frequency range (5–800 Hz) investigated.

The last precursor analyses the signal in function of the machine rotation instead of time, so it has been called angle domain precursor. As shown in the scheme of Fig. 6, for this precursor it is not enough to have a 5 s accelerometer signal, but it is necessary to have a tachometer signal acquired synchronously with the vibrational signal. So, the inputs of this precursor sub function include a 5 s tachometer signal which is an electric tension in function of time with an integer number of peaks for each turbine rotation. Counting the peaks, it is possible to divide both the signals into a set of intervals each lasting an integer number of rotations.

Once a set of intervals has been obtained, the function resamples them. So, each one has the same number of samples for the same number of rotation durations: the number of samples chosen is the maximum between those of all the intervals in the set; so, in all intervals no information is lost. The tachometer signal used for the software testing has the main content whose frequency is the double of the microturbine revolution speed. The signals used for the input came from some plant transitory from a stable condition to the surge. During this transient the machine speed was around 60 krpm (1000 Hz); so, each 5 s accelerometer signal entering the software loop has been divided into a set of intervals lasting 10 machine revolutions: inside of each interval it is possible to detect a minimum frequency of 100 Hz. After the creation of a set of consecutive intervals regarding the same number of rotations and with the same number of data points, these intervals are filtered in the range set by the user. The signal input of the software could refer to a machine regime with a different speed; so, the number of intervals inside the

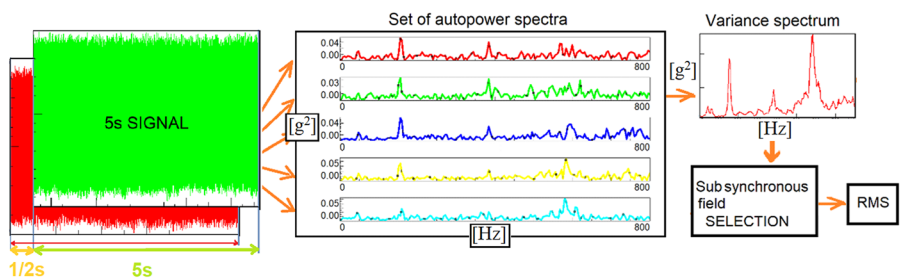

Fig. 5 Scheme of the precursor from variance spectrum

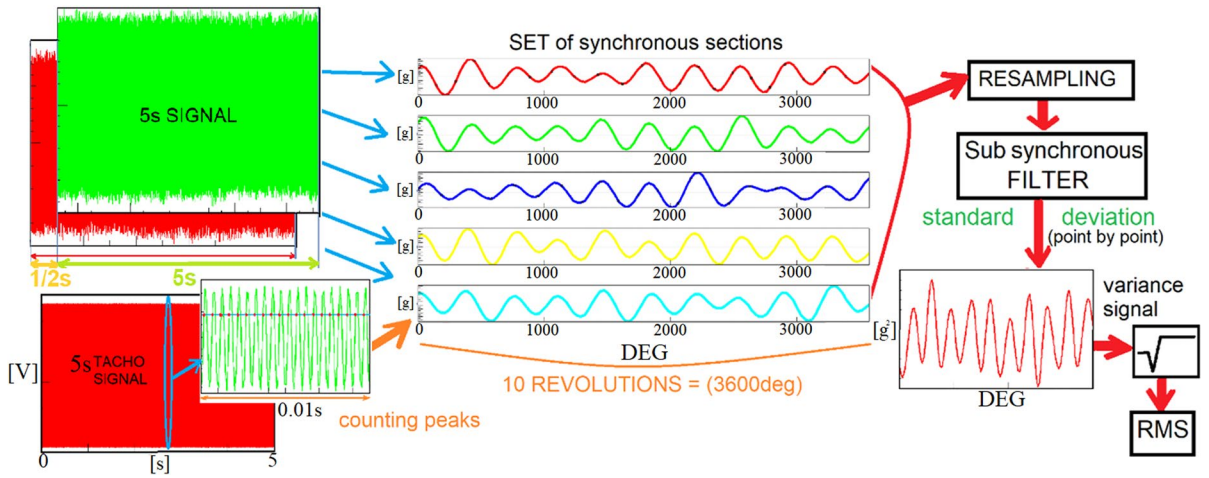

Fig. 6 Scheme of the precursor from angle domain analysis

calculated set could change: the software user has to define the number of intervals to be considered for the precursor calculation (based on the average machine speed during the acquisition). For the software testing, the calculation of the angle domain precursor was carried out considering 350 intervals of the set from the 5 s input and each interval was filtered between 5 to 800 Hz with a filter order of 10. Once the set has been prepared with a precise number of intervals of a precise number of rotations, the angle domain precursor is calculated. Initially, the software calculates the average interval adding up point by point all the intervals and dividing for their number and, then, it calculates point by point the variance signal from the mean. As Fig. 6 shows, the angle domain precursor is obtained calculating the RMS value of the variance signal (the signal points are the variance of all the corresponding points in the set). From the data used for software testing, the angle domain precursor value appears to be more floating than the other precursors; so, a sort of moving average has been implemented. Every half a second the main function takes into account not the value of the last calculated precursor, but the median value between the last one calculated and the two values calculated before.

6 Software tuning and results

As described before, the software developed has some parameters that can be set by the user: part of the work has been related to the correct selection of the default values for these parameters. Some values were chosen based on the previous analysis of vibro-acoustical signals [14, 39]. These are the above-mentioned parameters during the description of the precursor functions. However, the other parameters, regarding the reference calculation and their comparison with the actual precursor values, have been chosen through a tuning process.

In the past experimental campaign [39], tachometer, vibrational and acoustic signals were acquired from the test rig presented in Sect. 3. Signals were acquired considering transient trends from steady-state condition at about 60,000 rpm to the surge: these transients were obtained progressively closing a valve placed in the main air stream while the plant is equipped with one of these three volumes: 0.3 m^3, 2.3 m^3 and 4.1 m^3. The surge instability was reached closing the valve by steps of 10–5% from fully open condition to the surge event. Previous papers [14, 39] can be considered for an in-depth description of the transients and for the main results of plant performance.

Signals from transient tests have been used for the tuning process: to choose the best software parameters to predict the surge instability. The three signals from each transient were divided in a set of 5 s intervals with an overlap of 4.5 s between one interval and its previous one. These sets are useful to test the software because it is possible to simulate a real-time acquisition giving realistic data as input of the software (in

the form of 5 s intervals every ½ a second). Inserting data from different transients, parameters were chosen to obtain 3 or 4 warnings when the plant is in proximity of or during the surge condition, trying to avoid any false alarms (3 or 4 warnings far from surge conditions). After subsequent attempts, it was possible to obtain the default parameters in Table 1 useful for good surge prevention performance.

The results shown below are all obtained using the default parameters from the tuning process. These vibro-acoustic data used to assess the surge prevention software performance regard three tests obtained with the T100 test rig and already described in the previous paper [39] (one transient operation for each volume configuration). So, in [39] the reader can have access to the trends of the related plant properties during these three tests.

In each of Figs. 7, 8, 9 four graphs are represented: one for each precursor during the same transient to the surge condition (at time zero). The abscissa axis shows the time of the distance from surge. So, the left limit of the abscissa axis corresponds to the most stable condition plotted on the graphs. During the transients to surge, the time distance between one percentage valve closure to another might not be constant and the surge has been obtained in different

Table 1 Software default parameters defined in the tuning process

No. of precursor values for the reference matrix	15
Starting value for maximum time distance	50 half seconds
Time variation: automatic correction	10 half seconds
Threshold for accelerometer: sub-synchronous RMS	16%
Threshold for microphone: sub-synchronous RMS	14%
Threshold for variance spectrum: sub-synchronous RMS	16%
Threshold for angle domain analysis RMS	14%

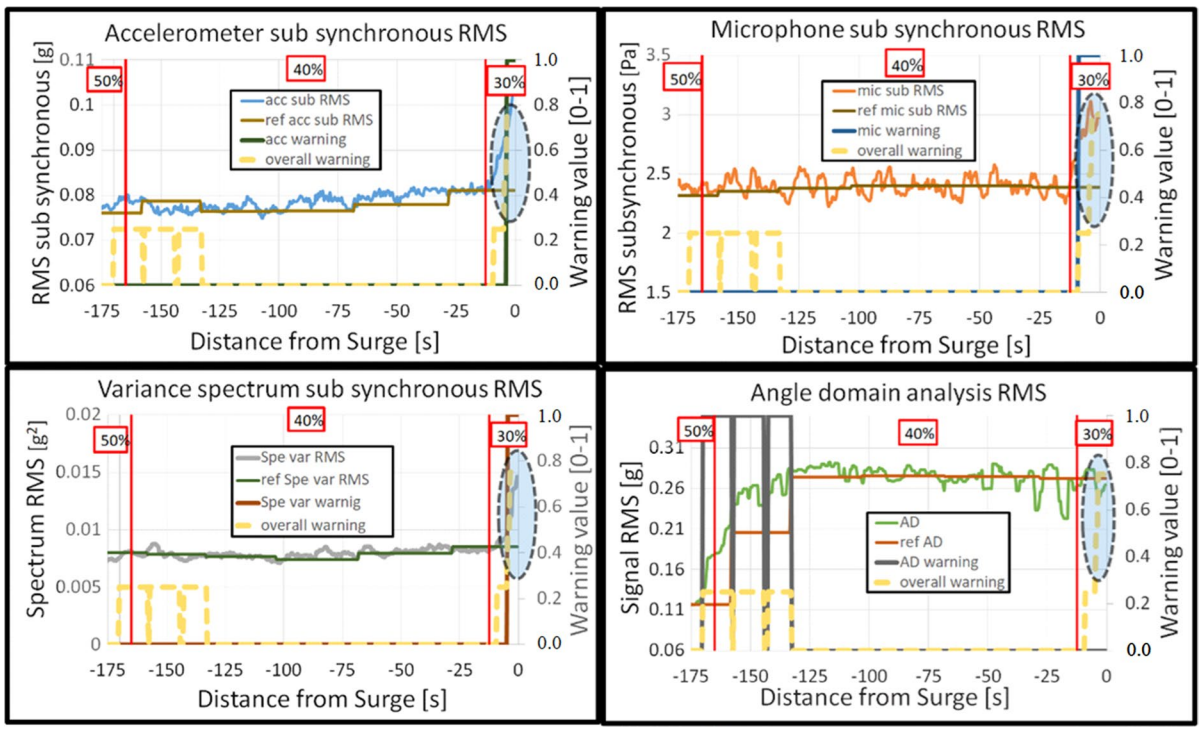

Fig. 7 Software results with 0.3 m^3 volume

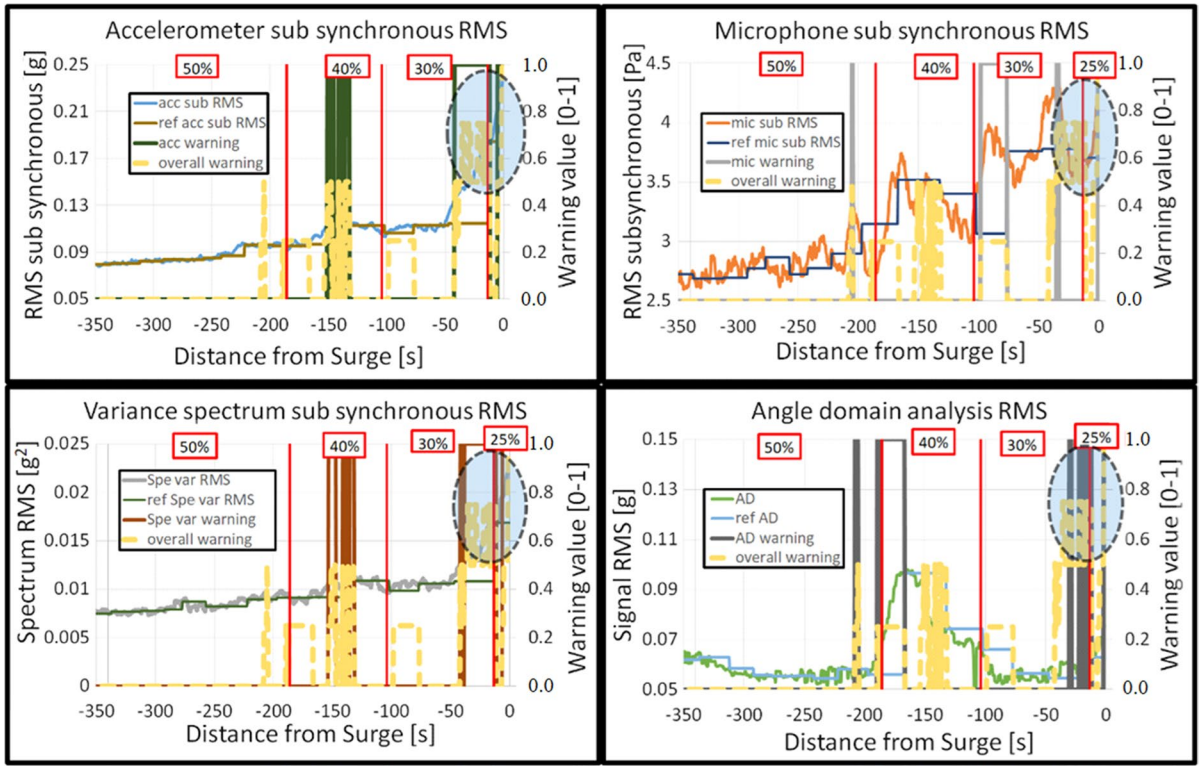

Fig. 8 Software results with 2.3 m^3 volume

closures: so, in the graphs red vertical lines separate the different valve conditions. Inside the red squares the picture provides an indication of the valve opening condition for each time interval between two red vertical lines.

In each graph of the figure there are two ordinate axes: the left one indicates the values of the precursor and the reference, while the axes on the right show the warning values. In the graphs, from the reference trend, it is possible to see the time intervals in which the reference value has been kept constant. Two warning values are plotted: the darker one is a Boolean (0 or 1) value which indicates whether the single precursor has (1) or not (0) crossed its threshold (if precursor actual value is higher than its reference value of the percentage indicated into the Table 1). Yellow dashed lines represent the overall warning value during the transient to the surge: it is calculated obtaining the mean of all four Boolean values from all the precursors. The overall warning signal can assume only 5 values (0.0, 0.25, 0.5, 0.75, 1.0), that correspond to the number of active warnings (from 0 to 4); an overall waning of 0.75 or higher can be considered as an alarm that means that the system is approaching a surge event.

Dashed circles in each graph indicate where the overall warning gives an alarm. As shown in the figures, in all three volume configurations the alarm appears some seconds before the surge in a valve condition around 30–25% opening. In Fig. 9 relative to the 4.1 m^3 case, an alarm is given farther from the surge than in the other figures; however, it appears at a similar valve closing, so in a similar plant status. After the alarm has been given, 3 of the 4 precursors tend to keep values higher than before the alarm; this means that the system is working in a less stable condition and the alarm is true.

In all three volume configurations, the alarm seems be able to predict the surge in time to permit the plant control system to operate to avoid the instability (e.g. opening a bleed valve or removing the instability cause).

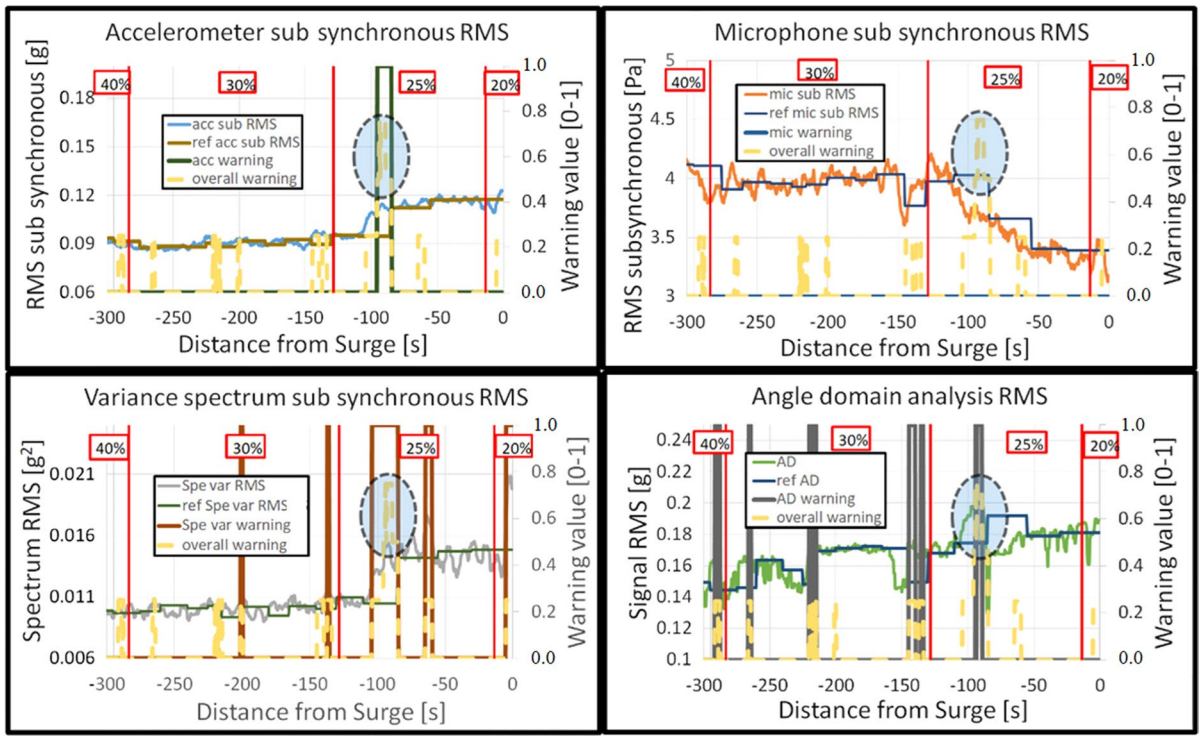

Fig. 9 Software results with of 4.1 m^3 volume

6.1 Preliminary software results from a different compressor and plant

To confirm the effectiveness of the developed software, it was also applied to the signals coming from a new experimental campaign on a different plant. The new plant is composed of an automotive turbocharger (Garrett GT1238Z) whose centrifugal compressor is very different in size, operative range, mass flow and pressure ratio than that of a T100 microturbine already analysed. However, as for the T100, this turbocharger is also connected to a large pressure vessel: it is equipped with a burner between the compressor and the expander, to operate the turbocharger as a gas turbine. A complete description of the system, that is not discussed here for the sake of brevity, is reported in [40]. Moreover, the exhaustive description of the experimental campaign is presented in [41]. Regarding the turbocharger compressors instability, the authors also suggest reading of Marelli's works [42].

In this sub-paragraph, one exemplary result of the collected data is presented. In details, Fig. 10, similarly to the other figures in paragraph 6, represents four graphs: one for each precursor during the same transient to the surge condition (at time zero). Also on this plant the surge unstable condition was obtained progressively closing a valve placed in the main air stream downstream of the turbocharger compressor (red squared percentages). Results in Fig. 10 are related to a transient starting from a stable operational condition of 207.2 krpm rotational speed, 43.5 g/s mass flow and 2.1 pressure ratio until the surge event was reached with a valve opening of 40%.

During the transient to the instability all the 4 precursor values (ordinate axis on the left) have a relevant increasing before the surge event. This behaviour is detected by the mobile threshold system which responds with individual and overall warnings (dashed circles). An important aspect to be underlined is that the software was able to warn the incipience of surge with a different compressor and a different plant considering the same parameters setting used for T100 compressor. This confirms the software effectiveness and flexibility.

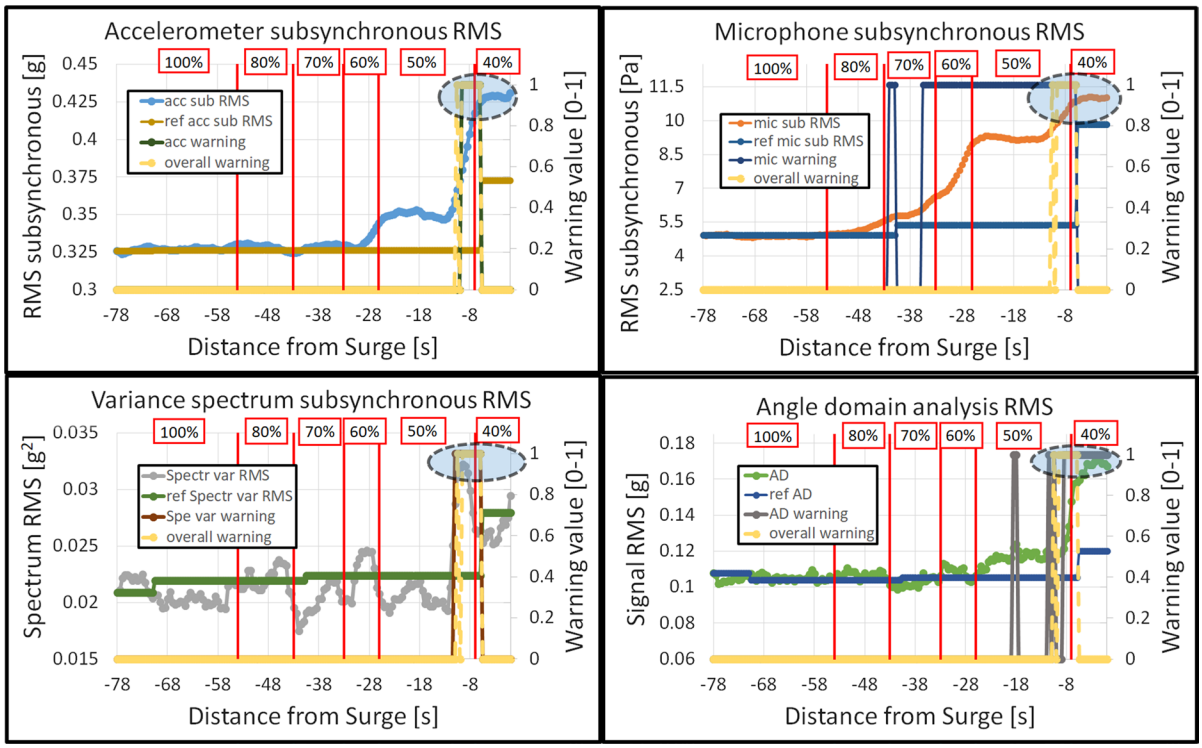

Fig. 10 Software results from the turbocharger-based plant

7 Conclusions

This paper shows the development of innovative software for the real-time prevention of surge conditions from vibro-acoustic measurements. Precursors implemented in a LabVIEW script are:

- the RMS energy value of the sub-synchronous frequency contents from both accelerometer and microphone signal;
- the accelerometer RMS value of the variance spectrum;
- and the RMS value of the signal variance calculated from set of signal sections lasting an integer number of machine rotations (angle domain analysis).

All these values are calculated by the software every half a second from a signal interval of five seconds and compared with the corresponding reference threshold. An important innovative aspect regards the reference value that is not constant to have flexibility for application with different machines and different operative conditions. So, this reference value is calculated from the precursor values obtained some second before and it changes after a certain time interval to different plant conditions and machine regimes. The tuning process, using data from a plant based on a T100 microturbine, reveals that a good threshold for surge prediction can be obtained considering the median of 15 values calculated by the software 50 half seconds before, with an automatic correction of this time distance of 10 half seconds. If three present values exceed their reference values of a chosen percentage, the system is considered close to surge condition.

The software has been tested with data from three T100 plant volume configurations (0.3 m^3, 2.3 m^3, 4.1 m^3) between turbine compressor outlet and recuperator inlet: the tool produced an alarm some seconds before the surge instability when the valve (causing the instability) was in the 25–30% range. So, the software was able to successfully predict the surge event in all the three volume conditions. Furthermore, tests on new data collected on a different compressor (different plant) confirm its effectiveness

and flexibility. Thanks to the application of this software, it will be possible to increase application range of innovative gas turbine cycles and, as consequence, the energy generation efficiency.

A possible future development of this surge prevention tool could include the application of a one-class machine learning algorithm. It could be trained by the precursor values obtained as results during the software test with past data [39] in a stable condition (far from the surge event). Regarding machine learning, authors suggest R. Camoriano's works [43], 44], while regarding one-class machine learning other papers [45], 46].

Acknowledgements A special acknowledgement is offered to Dr. Matteo Pascenti, laboratory, technician at TPG, for his activities in the experimental tests and Dr. Alberto Nicola Traverso, employed by H2Boat (spin-off of the University of Genoa), for his support in the software development.

Funding Open access funding provided by Università degli Studi di Genova within the CRUI-CARE Agreement.

Declarations

Conflict of interest The authors declare that they have no conflict of interest.

References

1. Guelpa E, Bischi A, Verda V, Chertkov M, Lund H (2019) Towards future infrastructures for sustainable multi-energy systems: a review. Energy 184:2–21
2. Radpour S, Hossain Mondal MA, Kumar A (2017) Market penetration modeling of high energy efficiency appliances in the residential sector. Energy 134:951–961
3. Jansohn P (2013) Modern gas turbine systems: high efficiency low emission fuel flexible power generation. Elsevier, Amsterdam
4. Lund H (2018) Renewable heating strategies and their consequences for storage and grid infrastructures comparing a smart grid to a smart energy systems approach. Energy 151:94–102
5. Wang R, Liu S, Li Q, Zhang S, Wang L, An S (2021) CO_2 capture performance and mechanism of blended amine solvents regulated by N-methylcyclohexyamine. Energy 215:119209
6. Fallah M, Siyahi H, Ghiasi RA, Mahmoudi SMS, Yari M, Rosen MA (2016) Comparison of different gas turbine cycles and advanced exergy analysis of the most effective. Energy 116:701–715
7. Ferrari ML, Traverso A, Pascenti M, Massardo AF (2007) Early start-up of solid oxide fuel cell hybrid systems with ejector cathodic recirculation: Experimental results and model verification. Proc Instf Mech Eng Part A: J Power Energy 221:627–635
8. Traverso A, Massardo AF (2002) Thermoeconomic analysis of mixed gas-steam cycles. Appl Therm Eng 22:1–21
9. Sheikhbeigi B, Ghofrani MB (2007) Thermodynamic and environmental consideration of advanced gas turbine cycles with reheat and recuperator. Int J Environ Sci Technol 4:253–262
10. Kayadelen HK, Ust Y (2017) Thermodynamic, environmental and economic performance optimization of simple, regenerative, STIG and RSTIG gas turbine cycles. Energy 121:751–771
11. Al-attab KA, Zainal ZA (2015) Externally fired gas turbine technology: a review. Appl Energy 138:474–487
12. Schrader AJ, Schieber GL, Ambrosini A, Loutzenhiser PG (2020) Experimental demonstration of a 5 kW_{th} granular-flow reactor for solar thermochemical energy storage with aluminum-doped calcium manganite particles. Appl Therm Eng 173:115257
13. Kim MJ, Kim TS (2019) Integration of compressed air energy storage and gas turbine to improve the ramp rate. Appl Energy 247:363–373
14. Reggio F, Ferrari ML, Silvestri P, Massardo AF (2019) Vibrational analysis for surge precursor definition in gas turbines. Meccanica 54:1257–1278
15. McDonald CF, Massardo AF, Rodgers C, Stone A (2008) Recuperated gas turbine aeroengines, part I: early development activities. Aircr Eng Aerosp Technol 80:139–157
16. Caratozzolo F, Ferrari ML, Traverso A, Massardo AF (2013) Emulator rig for SOFC hybrid systems: temperature and power control with a real-time software. Fuel Cells 13:1123–1130
17. Mohammed H, Al-Othman A, Nancarrow P, Tawalbeh M, El Haj Assad M (2019) Direct hydrocarbon fuel cells: a promising technology for improving energy efficiency. Energy 172:207–219
18. Lucifredi A, Giribone P, Ghirelli M, Silvestri P (2014) Analysis of the vibration behavior and evaluation of the fatigue life consumption of the structural elements of a tele-diagnostics device of an underground rail vehicle. In: 11th international conference on condition monitoring and machinery failure prevention technologies, CM 2014/MFPT 2014
19. Bardelli M, Cravero C, Marini M, Marsano D, Milingi O (2019) Numerical investigation of impeller-vaned

diffuser interaction in a centrifugal compressor. Appl Sci 9(8):1619
20. Cravero C, Marsano D (2020) Criteria for the stability limit prediction of high speed centrifugal compressors with vaneless diffuser. Part I: Flow structure analysis and Part II: The development of prediction criteria, ASME Turbo Expo 2020, ASME paper GT2020–14579 and GT2020–14589, London, UK, 22–26 June 2020
21. Arnulfi GL, Giannattasio P, Giusto C, Massardo AF, Micheli D, Pinamonti P (1999) Multistage centrifugal compressor surge analysis. Part I: Exp Investig J Turbomach 121:305–311
22. Arnulfi GL, Giannattasio P, Giusto C, Massardo AF, Micheli D, Pinamonti P (1999) Multistage centrifugal compressor surge analysis: Part II-numerical simulation and dynamic control parameters evaluation. J Turbomach 121:312–320
23. Fink DA, Cumpsty NA, Greitzer EM (1992) Surge dynamics in a free spool centrifugal compressor system. J Turbomach 114:321–322
24. Aretakis N, Mathioudakis K, Kefalakis M, Papailiou K (2004) Turbocharger unstable operation diagnosis using vibroacoustic measurements. ASME J Eng Gas Turbines Power 126:840–847
25. Fanyu L, Jun L. Stall warning approach with application to stall precursor-suppressed casing treatment. ASME Paper GT2016–58172, ASME Turbo Expo 2016, Seoul, South Korea
26. Morini M, Pinelli M, Venturini M. Acoustic and vibrational analyses on a multi-stage compressor for unstable behavior precursor identification. ASME Paper GT2007–27040, ASME Turbo Expo 2007, Montreal, Canada
27. Tan CS, Day I, Morris S, Wadia A (2010) Spike-type compressor stall inception, detection, and control. Annu Rev Fluid Mech 42:275–300
28. Hipple SM, Reinhart ZT, Bonilla-Alvarado H, Pezzini P, Bryden KM (2020) Using machine learning tools to predict compressor stall. J Energy Resour Technol 142:070915
29. Moen L (2010) Method and device for determining the occurrence of rotating stall in a compressor's turbine blade II. US Patent, N. 7,677,090 B2
30. Gopisetty S, Treffinger P, Reindl LM (2017) Open-source energy planning tool with easy-to-parameterize components for the conception of polygeneration systems. Energy 126:756–765
31. Henke M, Monz T, Aigner M (2017) Introduction of a new numerical simulation tool to analyze micro gas turbine cycle dynamics. J Eng Gas Turbine Power 139:042601
32. Qiu K, Yan L, Ni M, Wang C, Xiao G, Luo Z, Cen K (2015) Simulation and experimental study of an air tube cavity solar receiver. Energy Convers Manag 103:847–858
33. Montero CM, De Paepe W, Parente A, Contino F (2016) T100 mGT converted into mHAT for domestic applications: economic analysis based on hourly demand. Appl Energy 164:1019–1027
34. Zaccaria V, Tucker D, Traverso A (2016) Transfer function development for SOFC/GT hybrid systems control using cold air bypass. Appl Energy 165:695–706
35. Maia TAC, Barros JEM, Cardoso Filho BJ, Porto MP (2016) Experimental performance of a low cost micro-CAES generation system. Appl Energy 182:358–364
36. Mahmood M, Traverso A, Traverso AN, Massardo AF, Marsano D, Cravero C (2018) Thermal energy storage for CSP hybrid gas turbine systems: Dynamic modelling and experimental validation. Appl Energy 212:1240–1251
37. Aydin D, Casey SP, Riffat S (2015) The latest advancements on thermochemical heat storage systems. Renew Sustain Energy Rev 41:356–367
38. Sousa MS, Barbosa PCPF, Del Claro VTS, Nicoletti R, Cavalini AA, Steffen V (2021) Numerical prediction and experimental validation of an onboard rotor under bending. Meccanica 56:2631–2650
39. Ferrari ML, Silvestri P, Pascenti M, Reggio F, Massardo AF (2018) Experimental dynamic analysis on a T100 microturbine connected with different volume sizes. J Eng Gas Turbines Power 140:021701
40. Ferrari ML, Pascenti M, Abrassi A (2019) Test rig for emulation of turbocharged SOFC Plants. In: E3S Web of Conferences, vol 113, pp 02001
41. Silvestri P, Reggio F, Ferrari ML, Niccolini Marmont Du Haut Champ CA, Compressor surge precursors for a turbocharger coupled to a pressure vessel. In: Proceedings of the ASME Turbo Expo 2022 (in press)
42. Marelli S, Silvestri P, Usai V, Capobianco M (2019) Incipient surge detection in automotive turbocharger compressors (2019) SAE technical papers. https://doi.org/10.4271/2019-24-0186
43. Camoriano R, Traversaro S, Rosasco L, Metta G, Nori F. Incremental semiparametric inverse dynamics learning. In: 2016 IEEE international conference on robotics and automation (ICRA), pp 544–550
44. Camoriano R, Large-scale Kernel Methods and applications to lifelong robot learning. 2017 PhD Thesis
45. Cristianini N, Shawe-Taylor J (2000) An Introduction to support vector machines and other Kernel-based learning methods. Cambridge University Press, Cambridge
46. Schölkopf B, Williamson R, Smola A, Shawe-Taylor J, Platt J (2000) Support vector method for novelty detection. Solla SA, Leen TK, Müller K-R (eds), MIT Press, pp 582–588